Supplementary Information

Here we provide supplementary information about:

- ASTER mass balance spatial coverage
- Evaluation of individual glacier mass balance estimates
- Sensitivity to the choice of the glacier inventory
- Detailed comparison with ICESat estimates

ASTER mass balance spatial coverage

The ASTER DEMs were generated and processed based on 1°×1° tiles. Large parts of HMA are sparsely glacierized and the processing of one tile is computationally expensive (typically 4 days on a 6 core computing cluster), therefore we had to find a compromise between the needs in calculation resources and the area covered. For instance, there are many small glacierized catchments in the inner TP, which would have a very poor ratio in terms of computing time versus area of ice monitored. To optimize computing time, we calculated the cumulative distribution of glacierized area for all tiles (Figure S1), and computed the mass balance of the 130 most glacierized tiles, in order to estimate the volume change of more than 92 % of the glacierized area of HMA (Figure S1 and Table S3). We further added two extra tiles in Nyainqentanglha and inner TP with little glacier area but of specific interest. For the period 2000-2016, for each region, more than 75% of the sample area was retrieved (Table S3), with a decrease in the proportion of the sampling area with elevation, due to the greater occurrence of snow and consequently a lower visual contrast necessary for stereo parallax matching and thus elevation retrieval (Figure S2).

For a given tile/region/glacier, the volume change (and derived mass change) is calculated as the hypsometric average of elevation change. As a consequence for any regular grid, glaciers are sometimes split in between multiple tiles. For instance, in the endmember case of the large (~936 km²) Siachen Glacier in the eastern Karakoram, the accumulation area of the glacier is on one tile and the ablation area in another tile. Therefore, the gridded estimates are primarily intended to visualize the general pattern of elevation change – as the mass continuity condition is not fulfilled for parts of a glacier, where a change in surface elevation can be the consequence of either ice dynamics or a mass balance signal. For our regional estimates, glaciers are not split. The estimates are thus similar to glacier-wide mass balance as the ice dynamics effects cancel out. Note that the restriction to glaciers > 2 km^2 is only valid for our mass balance estimates for individual glaciers, in order to ensure sufficient

sampling of each hypsometric band within the small area of a single glacier. For the tile-/region-based estimates, glaciers smaller than 2 km² also contribute to the tile-/region-averaged mass balance.

Evaluation of individual glacier mass balance estimates

We limited the comparison to glaciers larger than 2 km² because glaciers smaller than this size have, in most cases, an uncertainty higher than ± 0.35 m w.e. yr^{-1} (see uncertainty assessment in the Method Section, all uncertainties are given at the 1 sigma confidence level).

For validation of our ASTER-based results, we use elevation change maps derived from SPOT5 (2003 in the Abramov Glacier area, 2005 for the Gangotri and Chhota Shigri regions) and Pléiades (2015 for the Abramov area and 2014 for the Gangotri and Chhota Shigri regions) DEMs (Figure S4 and S5).The methodology followed to compute the SPOT5 and Pléiades DEMs, to adjust them horizontally and vertically on the stable terrain, and to estimate the glacier-wide MB has been described in detail in ref. 1 for similar datasets acquired over the Mont Blanc area, European Alps. The uncertainties were estimated over Mont Blanc glaciers using repeated field GPS measurements[1]. Elevation changes from SPOT5/Pléiades DEM differencing were found to be accurate within ± 1.3 m and this error level was conservatively multiplied by a factor of 5 for regions where at least one of the DEMs had data gaps[1]. We converted volume change to glacier-wide MB using a conversion factor of 850 ± 60 kg m^{-3} (ref. 2).

The only glaciological mass balance series published in HMA that is long enough to be comparable to our data is the Chhota Shigri series[3]. For the 2005-2014 period, the glaciological annual mass balance was -0.41 ± 0.40 m w.e. yr^{-1} and the geodetic mass balance was initially estimated at -0.40 ± 0.28 m w.e. yr^{-1} (ref. 3). The SPOT5/Pléiades map of elevation change used to calculate the geodetic mass balance in ref. 3 exhibits a suspicious increase of thinning for elevations above 5000 m a.s.l. (black dashed line in Figure S5b), which biased the glacier-wide mass balance towards too negative values. The geodetic mass balance was thus recomputed using a new Pléiades stereo-pair acquired 26 September 2014, nearly at the exact same time of year as the SPOT5 stereo pair (20 and 21 September 2005). Thus no seasonal correction was applied. The curvature correction[4] had been neglected in ref. 3 and is now applied. The revised SPOT5-Pléiades elevation changes are in much better agreement with the ASTER results (red crosses in Figure S5b). The new glacier wide mass balance of Chhota Shigri Glacier using SPOT5-Pléiades is -0.23 ± 0.28 m w.e. yr^{-1} versus -0.27 ± 0.13 m w.e. yr^{-1} for ASTER.

Sensitivity to the choice of the glacier inventory

We calculate the mean rates of elevation change based on the ICIMOD glacier inventory[5] and the CCI glacier inventory for Karakoram[6] to test the sensitivity of our results to the inventory type and quality. The ICIMOD glacier inventory covers about 30,000 km² of ice in total. In the Karakoram, it results in 6.1 % less glacier area than the GAMDAM glacier inventory for the same region. The glacier volume change calculated on the ICIMOD glacier inventory is 8.8 % smaller than the volume change calculated based on the GAMDAM glacier inventory. The CCI glacier inventory for Karakoram covers about 22,000 km². This is 15.4 % larger than GAMDAM for the same region. The glacier volume change calculated based on the CCI glacier inventory is 7.1 % smaller than the volume change calculated based on the GAMDAM glacier inventory. The differences between the inventories are mainly due to varying acquisition dates of the underlying satellite imagery and different, but valid choices for glacier delineations[7]. This suggests that the uncertainty in volume change is not completely independent from the glacier area and definition of a glacier, as often assumed in the literature. However, the influence of the area considered on the volume change calculation is not straightforward to assess as it depends on the sensitivity of the mean rate of elevation change to the area change and on the sign of the mean rate of elevation change. As we do not have means to understand this complex response, we use an uncertainty of 10% on area, which is larger than the widely-used value of 5% from ref. 8, and we still assume that the uncertainties on the mean rate of elevation change and the uncertainty on area are independent. To our knowledge, no multi-temporal glacier inventory is available for entire HMA. Therefore, we assumed a constant glacierized area, and that variations in area are covered by our 10% area uncertainty.

Additionally, we provide estimates of glacier mass changes for the regions and glacier mask defined in Randolph Glacier Inventory[9] (Table S5).

Detailed comparison with ICESat estimates

For most regions, we found a good agreement between ICESat and ASTER mass change estimates (Table S4 and S5). However, significant differences exist for five controversial regions, i.e. Bhutan, Hindu Kush, Nyainqentanglha, Pamir Alay and Pamir. To understand these differences, we test three hypotheses: H1- ICESat scarce spatial sampling introduces bias; H2- the glacier mass balance changed between the early 2000s and recent years; H3- some regions have higher inter-annual variability of mass balance, to which the short ICESat acquisition period of five years only and the annually varying sample distribution might be sensitive to.

- To test H1, i.e. the representativeness of ICESat sampling, we extracted the ASTER elevation trends at the footprint locations only. The ASTER points were extracted in a circle of 70 m radius around the ICESat footprint center. This 70 m radius of the circle (twice as large as the

35 m radius of the ICESat footprint) was chosen as a compromise to average over enough ASTER DEM points so that the noise level is acceptable, and to average not over too many pixels to avoid contamination from pixels belonging to different area (e.g. from off-glacier terrain). As a consequence, the mean rate of elevation change for 16 to 21 ASTER pixels was assigned to each individual ICESat footprint on a glacier. From this collection of rates of elevation changes, we calculated the region-wide glacier mass balance by two means: 1- by calculating the mean elevation changes for each 100 m elevation band (area weighted or hypsometric average); 2- by calculating the dh for each point (dh is defined as the retrieved value of elevation extracted from an averaged ASTER trend at the date of ICESat acquisition, minus the SRTM elevation) and then fitting a robust trend of elevation change (completely analogous to ref. 10). Results obtained with both methods are shown in Table S1. It is not straightforward to estimate uncertainties for these retrieved values because ASTER elevations are much noisier than ICESat elevations at a given location. The resulting numbers are in very good agreement with the estimates calculated from the whole ASTER dataset (Table S1 and Table 1). This confirms that the spatial sampling of ICESat is adequate to represent the entire regions, at least for the entire ASTER period (2000-2016).

- To test H2, i.e. temporal shift in mass balances, we calculate the mass balance for the sub-periods 2000-2008 and 2008-2016 from ASTER DEMs. For these shorter sub-periods, the final number of available and retained DEMs is lower, and therefore uncertainties on these estimates are higher (see Method section). We observe no consistent shift in mass balances between the two periods (Table S2) that would help explaining the difference to the ICESat-based results. Unfortunately, estimates based on the 2003-2008 ASTER data only are too noisy, forcing us to limit this test to the 2000-2008 period that does not directly compare to the ICESat period.

- To test H3, spatio-temporal variability in mass balances, we explored the distribution of de-trended ICESat dh (ICESat–SRTM; Figure S10). For the non-controversial regions, the absolute value of the annual median of the de-trended dh is always below 1 m (the only exception is East Nepal in 2008), whereas it is often over 1 m and sometimes larger than 2 m for the controversial regions (Figure S10). In principle, high deviation of the median dh of one ICESat campaign indicates especially positive/negative glacier mass balance for that particular year, but the deviation could also be caused by bias in the ICESat or SRTM elevation data, a different hypsometry sampling biased towards tongues (typically stronger thinning) or accumulation areas (rather stable surface elevations), or snow fall right before ICESat's surface elevation sampling[11]. Bias is more likely for regions/campaigns with few ICESat samples. The

controversial regions have rather lower ICESat samples (<5,000 footprints; Table S1) spread over regions of similar size as the non-controversial regions. The regions may consist of different topo-climatic sub-regions that react differently to climate change. However, Figure 2b shows that a high (small) intra-regional dispersion in glacier-wide mass balances alone does not suffice as an indicator for (non-) controversial regions. To further test the potential influence of the inter-annual variability of glacier mass balance for the period 2003-2008, we calculated robust fits of elevation trends for the ICESat data in different configurations. First, we calculated the fit through the entire dataset for each region. Second, we removed one year of acquisition and fitted the trend to the remaining data. This was repeated for all six individual years from 2003 to 2008. The results are presented in Figure S11c, where each dot represents a fit with one year removed and the thick diamonds the fit which includes all six ICESat years. In this bootstrap test, all five controversial regions showed very high sensitivity to the removal of one year of data, contrary to the other regions (Figure S11c). They are especially highly sensitive to the removal of the first (2003) and last (2008) year of acquisition. In particular for Pamir, the year 2008 appears to be very dry[12,13]. Also for Abramov Glacier in Pamir Alay, ref. 14 found particularly negative values for 2008 in their reconstructed mass balance series. A particularly negative mass balance in 2008 could explain the negative trend in ICESat for these regions, where ASTER data suggest nearly balanced conditions.

We conclude that the sparse ICESat sampling used to derive region-wide mass balances in HMA from 2003 to 2008 is spatially representative, but when addressing longer-term processes (the data are often used for sea level rise estimates), it should be kept in mind that the mass balance calculated from ICESat trends are only valid within the short (5-year) monitoring period. They cannot be extrapolated to longer periods, in particular for these five regions.

Table S1: rate of glacier elevation change from ASTER trends [2000-2016] resampled with ICESat sampling.

Region	Mean rate of elevation change [m yr^{-1}], from hypsometric average	Robust linear trend of elevation [m yr^{-1}] from point cloud fit	Number of ICESat samples
Bhutan	-0.36	-0.29	1849
East Nepal	-0.39	-0.36	3990
Hindu Kush	-0.16	-0.24	3442
Inner TP	-0.14	-0.12	11467
Karakoram	-0.07	-0.03	14396
Kunlun	+0.20	+0.21	9543
Nyainqentanglha	-0.60	-0.58	3423
Pamir Alay	0.00	-0.07	920
Pamir	-0.06	-0.03	4260
Spiti-Lahaul	-0.39	-0.39	7579
Tien Shan	-0.23	-0.26	9619
West Nepal	-0.31	-0.30	4330

Table S2: region-wide mass balance for ASTER sub-periods

	ASTER MB [2000 – 2008]	**ASTER MB [2008 – 2016]**
	[m w.e. yr^{-1}]	**[m w.e. yr^{-1}]**
Bhutan	-0.31 ± 0.20	-0.50 ± 0.23
East Nepal	-0.32 ± 0.20	-0.22 ± 0.20
Hindu Kush	-0.14 ± 0.19	-0.05 ± 0.19
Inner TP	-0.01 ± 0.19	-0.24 ± 0.20
Karakoram	-0.06 ± 0.19	0.05 ± 0.19
Kunlun	0.24 ± 0.20	0.05 ± 0.19
Nyainqentanglha	-0.32 ± 0.22	-0.55 ± 0.26
Pamir Alay	-0.07 ± 0.19	-0.03 ± 0.19
Pamir	-0.04 ± 0.19	0.05 ± 0.20
Spiti-Lahaul	-0.49 ± 0.22	-0.11 ± 0.19
Tien Shan	-0.24 ± 0.20	-0.11 ± 0.20
West Nepal	-0.44 ± 0.21	-0.18 ± 0.20
Total	-0.15 ± 0.03	-0.11 ± 0.02

Table S3: summary of the sampled area and percentage of valid data for each sub period

Region	Total glacierized area [km²]	Sampled area [km²]	Percentage of sampled area	Percentage of valid data within the sampled area (2000-2016)	Percentage of valid data within the sampled area (2000-2008)	Percentage of valid data within the sampled area (2008-2016)
Bhutan	2291	1957	85.4	88	76.9	62.2
East Nepal	4776	4708	98.6	89.9	78.6	67.1
Hindu Kush	5147	5008	97.3	89.3	80.5	68
Inner TP	13102	9104	69.5	81.5	61.1	66.1
Karakoram	17734	17734	100.0	81.9	62.2	69.6
Kunlun	9912	9582	96.7	77.5	64.5	59.5
Nyainqentanglha	6378	6052	94.9	75	38.4	51.9
Pamir Alay	7167	7015	97.9	85.4	75.9	73.2
Pamir	1915	1665	86.9	89.1	78.8	54.2
Spiti-Lahaul	7960	7633	95.9	90.7	75.6	72.5
Tien Shan	10802	9832	91.0	87.9	80.8	44.6
West Nepal	4806	4787	99.6	89.4	75.2	61.6
Total	91990	85077	92.5	84.1	68.3	63.2

Table S4: Previously published region-wide mass balance estimates for HMA. For ICESat and GRACE based studies we do not provide the areas covered, as they do not correspond directly to the sampled areas. In the "comments" column, we point to some of the characteristics or weakness of the earlier estimates.

Region	MB [m w.e. yr^{-1}]	MB [Gt yr^{-1}]	Period	Area covered [km^2]	Study	Comments
Bhutan	-0.42 ± 0.33	-1.0 ± 0.8	2000-2016	2300	This study	
	-0.76 ± 0.20	-	2003-2008	-	Kääb et al., 2015 [10]	
	-0.22 ± 0.13	-	1999-2010	1380	Gardelle et al., 2013 [15]	SRTM
East Nepal	-0.33 ± 0.32	-1.6 ± 1.5	2000-2016	4780	This study	
	-0.31 ± 0.14	-	2003-2008	-	Kääb et al., 2015 [10]	
	-0.26 ± 0.13	-	1999-2011	1460	Gardelle et al., 2013 [15]	SRTM
	-0.79 ± 0.52	-	2002-2007	50	Bolch et al., 2011 [16]	Partial sampling
	-0.40 ± 0.25	-	2000-2008	200	Nuimura et al., 2012 [17]	
	-0.52 ± 0.22	-	2000-2016	N/A	King et al., 2017 [18]	SRTM
Hindu Kush	-0.12 ± 0.14	-0.6 ± 0.7	2000-2016	5150	This study	
	-0.42 ± 0.18	-	2003-2008	-	Kääb et al., 2015 [10]	
	-0.12 ± 0.16	-	1999-2008	800	Gardelle et al., 2013 [15]	SRTM
Inner TP	-0.14 ± 0.14	-1.8 ± 1.8	2000-2016	13100	This study	
	-0.06 ± 0.06	-	2003-2008	-	This study	ICESat
	0.02 ± 0.30	-	2003-2008	-	Neckel et al., 2014 [19]	average of their regions B, C, D E, F
Karakoram	-0.03 ± 0.14	-0.5 ± 2.5	2000-2016	17700	This study	
	-0.09 ± 0.12	-	2003-2008	-	Kääb et al., 2015 [10]	
	0.11 ± 0.22	-	1999-2008/2010	10750	Gardelle et al., 2013 [15]	SRTM
	-0.08 ± 0.12	-	2000-2012	1110	Rankl and Braun, 2016 [20]	STRM/TanDEM-X
Kunlun	0.14 ± 0.14	1.4 ± 1.4	2000-2016	9910	This study	
	0.18 ± 0.14	-	2003-2008	-	This study	ICESat
Nyainqentanglha	-0.62 ± 0.35	-4.0 ± 2.2	2000-2016	6380	This study	
	-1.14 ± 0.58	-	2003-2008	-	Kääb et al., 2015 [10]	
	-0.83 ± 0.57	-	2000-2014	280	Neckel et al., 2017 [21]	STRM/TanDEM-X
Pamir Alay	-0.08 ± 0.14	-0.6 ± 1.0	2000-2016	1910	This study	
	-0.59 ± 0.27	-	2003-2008	-	This study	ICESat
Pamir	-0.04 ± 0.14	-0.1 ± 0.3	2000-2016	7170	This study	
	-0.41 ± 0.24	-	2003-2008	-	Kääb et al., 2015 [10]	
	0.14 ± 0.13	-	1999-2011	3180	Gardelle et al., 2013 [15]	SRTM
Spiti Lahaul	-0.37 ± 0.15	-2.9 ± 1.2	2000-2016	7960	This study	
	-0.42 ± 0.26	-	2003-2008	-	Kääb et al., 2015 [10]	
	-0.45 ± 0.13	-	1999-2011	2110	Gardelle et al., 2013 [15]	SRTM
	-0.55 ± 0.37	-	2000-2012	1710	Vijay and Braun, 2016	STRM/TanDEM-X
Tien Shan	-0.28 ± 0.32	-3.0 ± 3.5	2000-2016	10800	This study	
	-0.37 ± 0.31	-	2003-2008	-	This study	ICESat
	-0.23 ± 0.19	-	2000-2009	3000	Pieczonka et al., 2013 [22]	
	-	-5.4 ± 2.8	2003-2009	-	Farinotti et al., 2015 [29]	GRACE-ICESat-Modelling

	-	-3.4 ± 0.8	2003-2009	-	Yi et al., 2016 [30]	ICESat
	-	-4.0 ± 0.7	2003-2014	-	Yi et al., 2016 [30]	GRACE
West Nepal	-0.34 ± 0.15	-1.6 ± 0.7	2000-2016	4810	This study	
	-0.37 ± 0.15	-	2003-2008	-	Kääb et al., 2015 [10]	
	-0.32 ± 0.13	-	1999-2011	910	Gardelle et al., 2013 [15]	SRTM

Table S5: region-wide mass balances from ASTER (2000-2016) calculated on RGI inventory and RGI regions[9]

RGI regions	Region ID	MB ASTER 2000-2016 [m w.e. yr-1]	MB ASTER 2000-2016 [Gt yr-1]
Hissar Alay	13_01	-0.04 ± 0.07	-0.1 ± 0.1
Pamir	13_02	-0.06 ± 0.07	-0.6 ± 0.7
W Tien Shan	13_03	-0.20 ± 0.08	-1.9 ± 0.7
E Tien Shan	13_04	-0.40 ± 0.20	-1.1 ± 0.5
W Kun Lun	13_05	0.16 ± 0.08	1.3 ± 0.6
E Kun Lun	13_06	-0.01 ± 0.07	0.0 ± 0.2
Qilian Shan	13_07	-0.29 ± 0.08	-0.5 ± 0.1
Inner Tibet	13_08	-0.19 ± 0.08	-1.5 ± 0.5
S and E Tibet	13_09	-0.55 ± 0.23	-2.2 ± 0.8
Hindu Kush	14_01	-0.13 ± 0.07	-0.4 ± 0.2
Karakoram	14_02	-0.03 ± 0.07	-0.6 ± 1.7
W Himalaya	14_03	-0.38 ± 0.09	-3.0 ± 0.7
C Himalaya	15_01	-0.28 ± 0.08	-1.5 ± 0.5
E Himalaya	15_02	-0.38 ± 0.20	-1.9 ± 0.9
Hengduan Shan	15_03	-0.56 ± 0.23	-2.5 ± 1.0

Table S6: comparison of region-wide mass balances values obtained by Gardner et al. (ref. 23) for 2003-2009 and with ASTER for 2000-2016

Region ID	MB from ref. 23 2003-2009 [m w.e. yr^{-1}]	MB ASTER 2000-2016 [m w.e. yr^{-1}]
Pamir Hissar Alay	-0.12 ± 0.24	-0.06 ± 0.07
Tien Shan	-0.52 ± 0.24	-0.25 ± 0.11
W Kun Lun	+0.16 ± 0.18	+0.16 ± 0.08
E Kun Lun and Inner TP	-0.01 ± 0.15	-0.14 ± 0.08
Qilian Shan	-0.29 ± 0.33	-0.29 ± 0.08
S and E Tibet	-0.27 ± 0.16	-0.55 ± 0.23
Karakoram et Hindu Kush	-0.10 ± 0.18	-0.04 ± 0.07
W Himalaya	-0.48 ± 0.17	-0.38 ± 0.09
C Himalaya	-0.40 ± 0.23	-0.28 ± 0.08
E Himalaya	-0.80 ± 0.22	-0.38 ± 0.20
Hengduan Shan	-0.36 ± 0.43	-0.56 ± 0.23

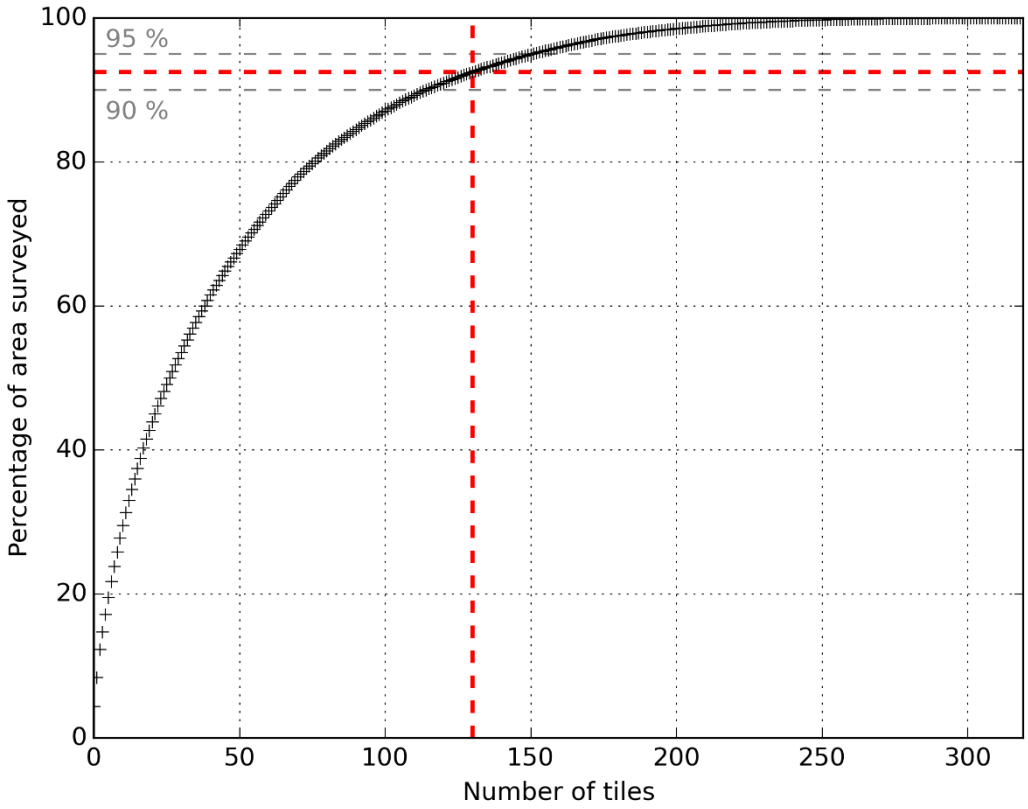

Figure S1: cumulative distribution of glacierized area as a function of the number of tiles considered (sorted in descending order). For the 130 most glacierized tiles, we reach a total percentage of 92 % (red dashed lines).

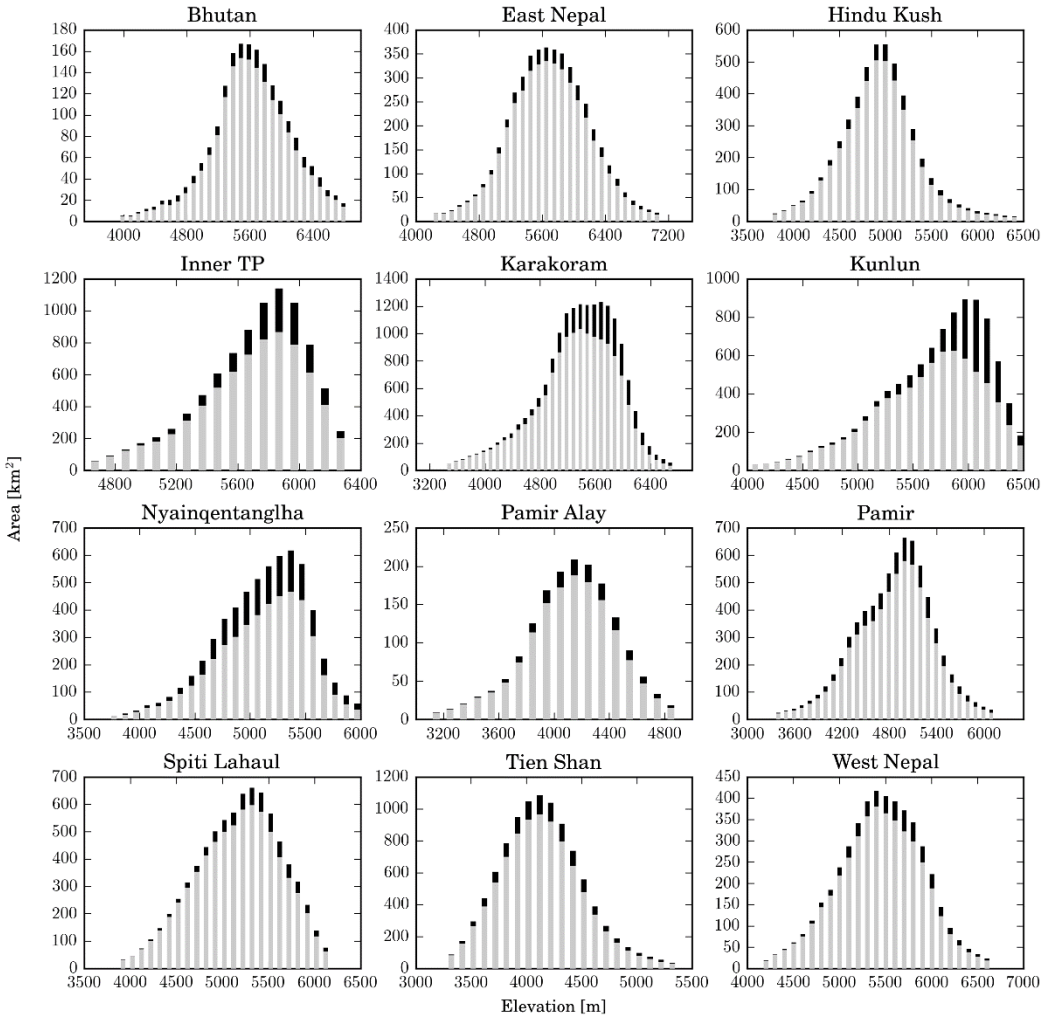

Figure S2: hypsometry of the 12 surveyed regions. The black bars represent the total area and the grey superimposed bars the area for which data considered as valid were obtained from ASTER DEMs for the period 2000-2016.

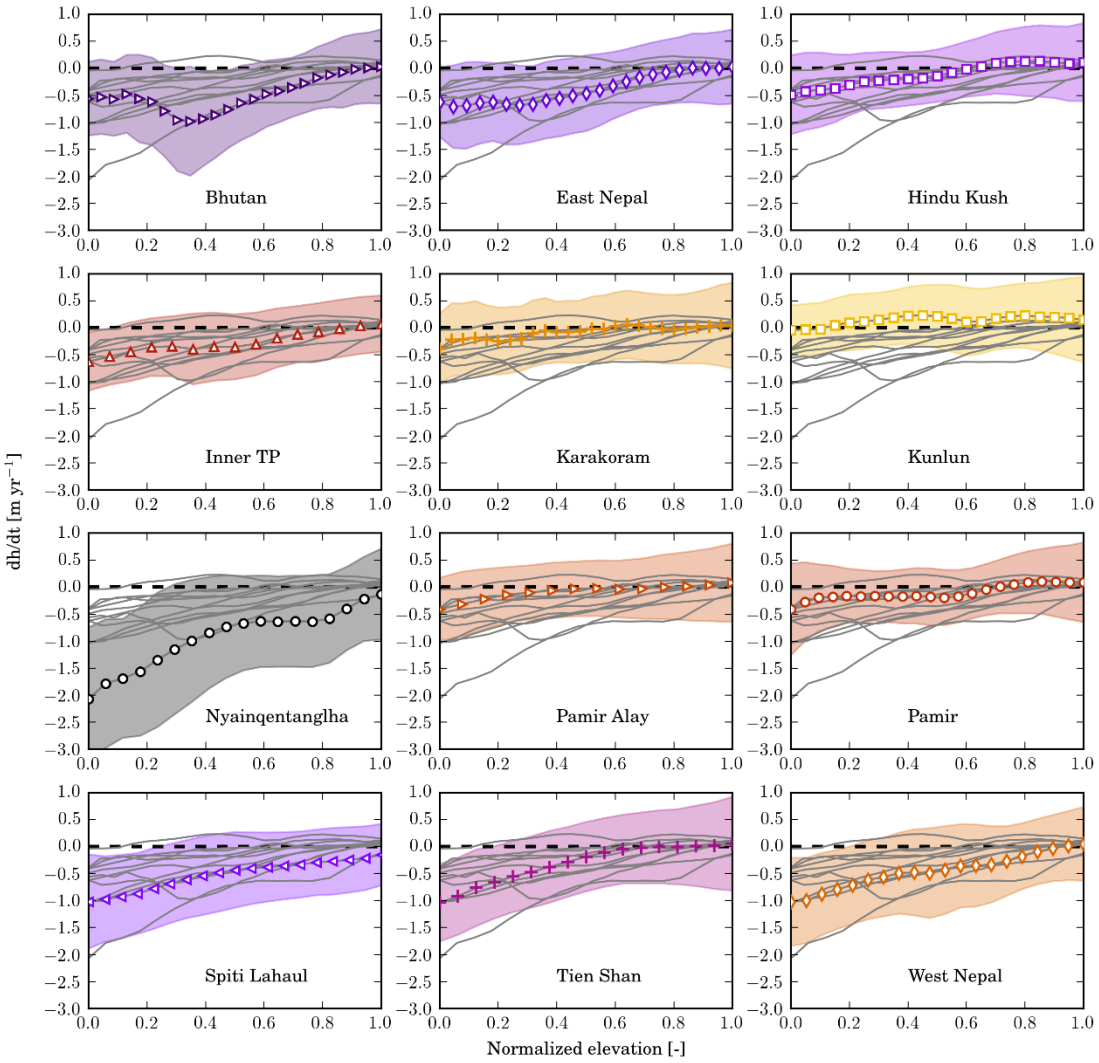

Figure S3: rate of elevation change as a function of normalized elevation. For each panel, the shaded area represents the mean of rate of elevation change ± 1 NMAD. The grey curves represent the other regions, for comparison.

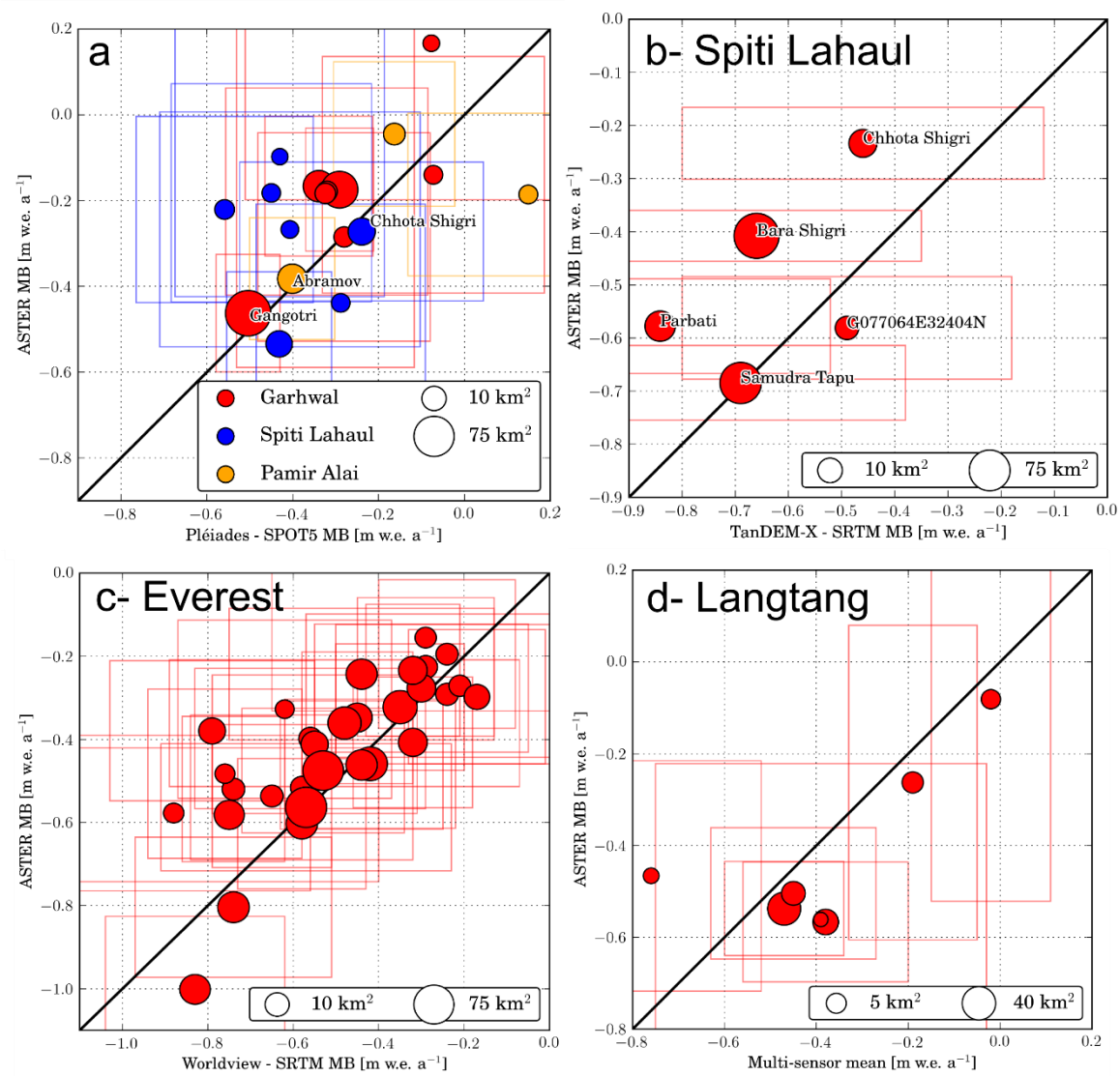

Figure S4: Glacier-wide estimates from ASTER method versus estimates for the same glaciers using multiple Pléiades - SPOT5 DEM differences (a), TanDEM-X – SRTM differences (b- the mass balance estimates and uncertainties come from ref. 24), Worldview – SRTM differences (c- the mass balance estimates and uncertainties come from ref. 18), multiple sensor elevation difference (d- the mass balance estimates and uncertainties come from ref. 25). The thick line is the 1:1 line. The rectangles represent the error bars associated with the two methods. The location of these validation sites are shown by yellow triangles in Figure 1.

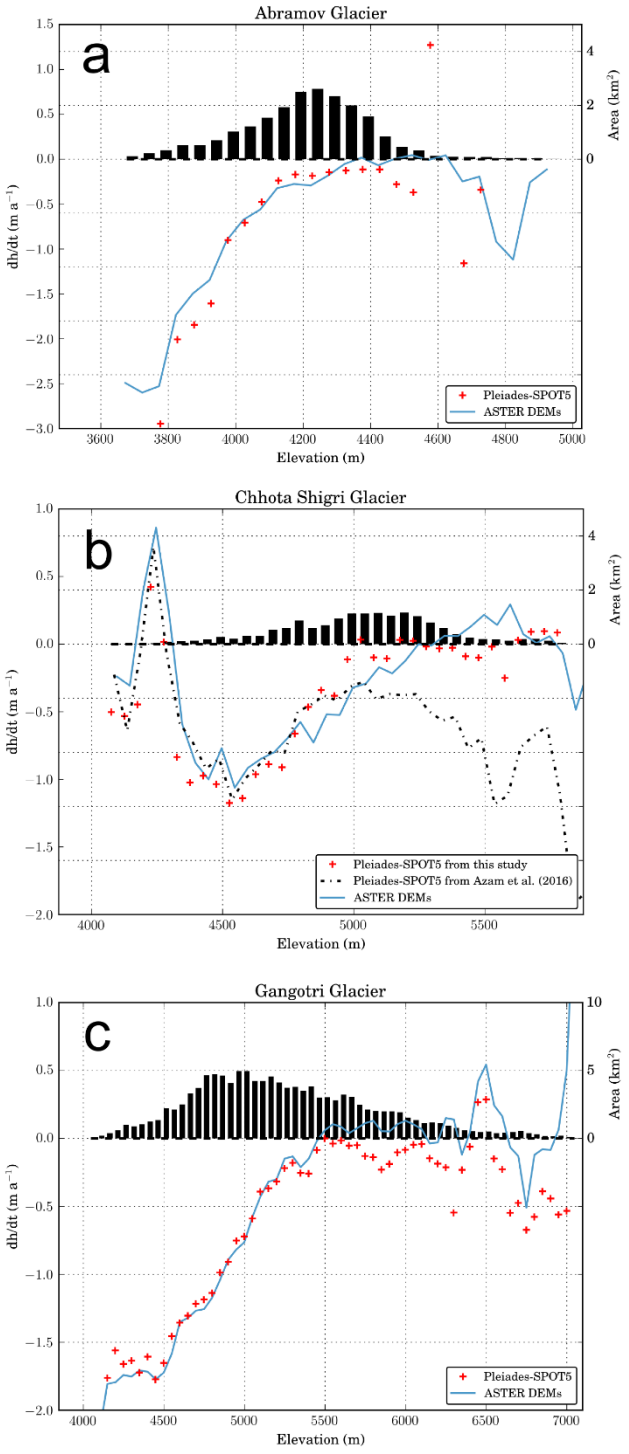

Figure S5: rate of elevation change for a- Abramov Glacier (Pamir Alay) derived from a Pléiades - SPOT 5 difference (images acquired in Aug. 2003 and Sept. 2015), b- Chhota Shigri Glacier (Spiti Lahaul) derived from a Pléiades - SPOT 5 difference (images acquired in Sept. 2005 and Sept. 2014), c- Gangotri Glacier (Garhwal) derived from a Pléiades - SPOT 5 difference (images acquired in Nov. 2004 and Aug. 2014) and from ASTER DEMs for the same periods.

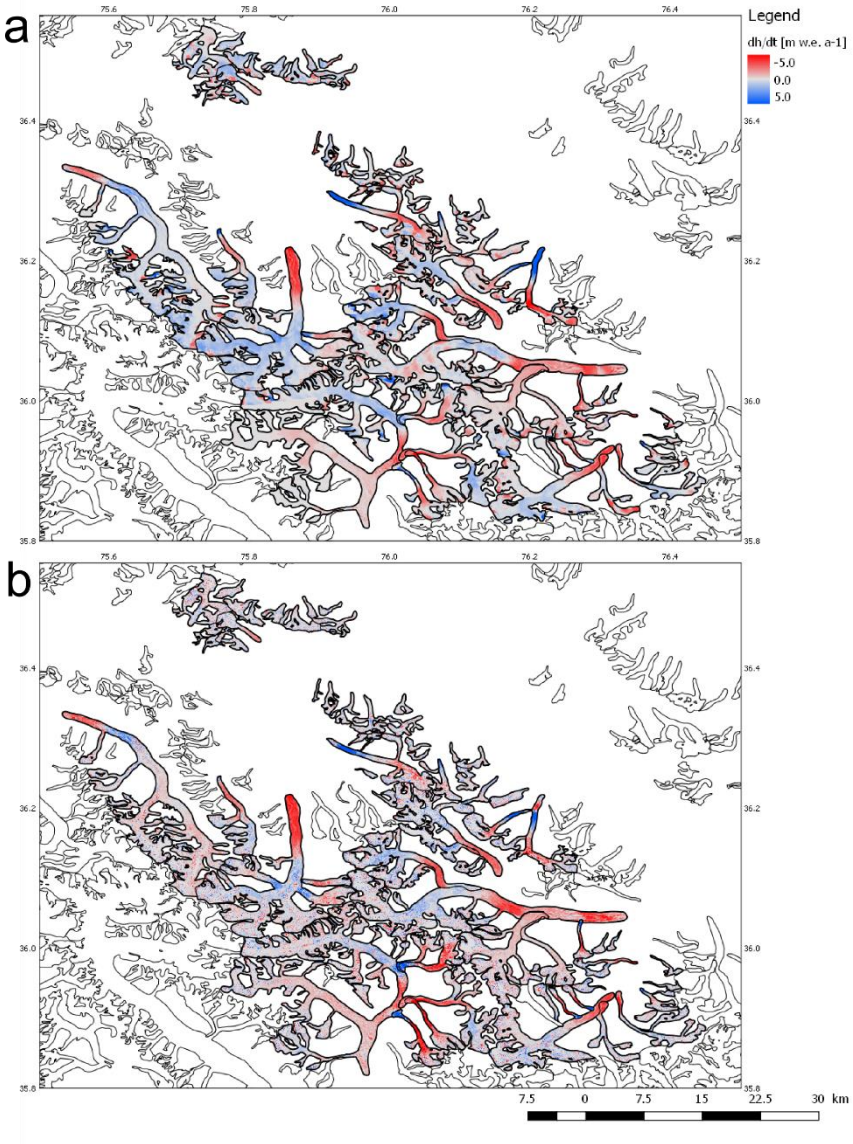

Figure S6: map of elevation change [m yr^{-1}] for the period 2000-2012 over central Karakoram from ref. 20 (a) and from this study (b).

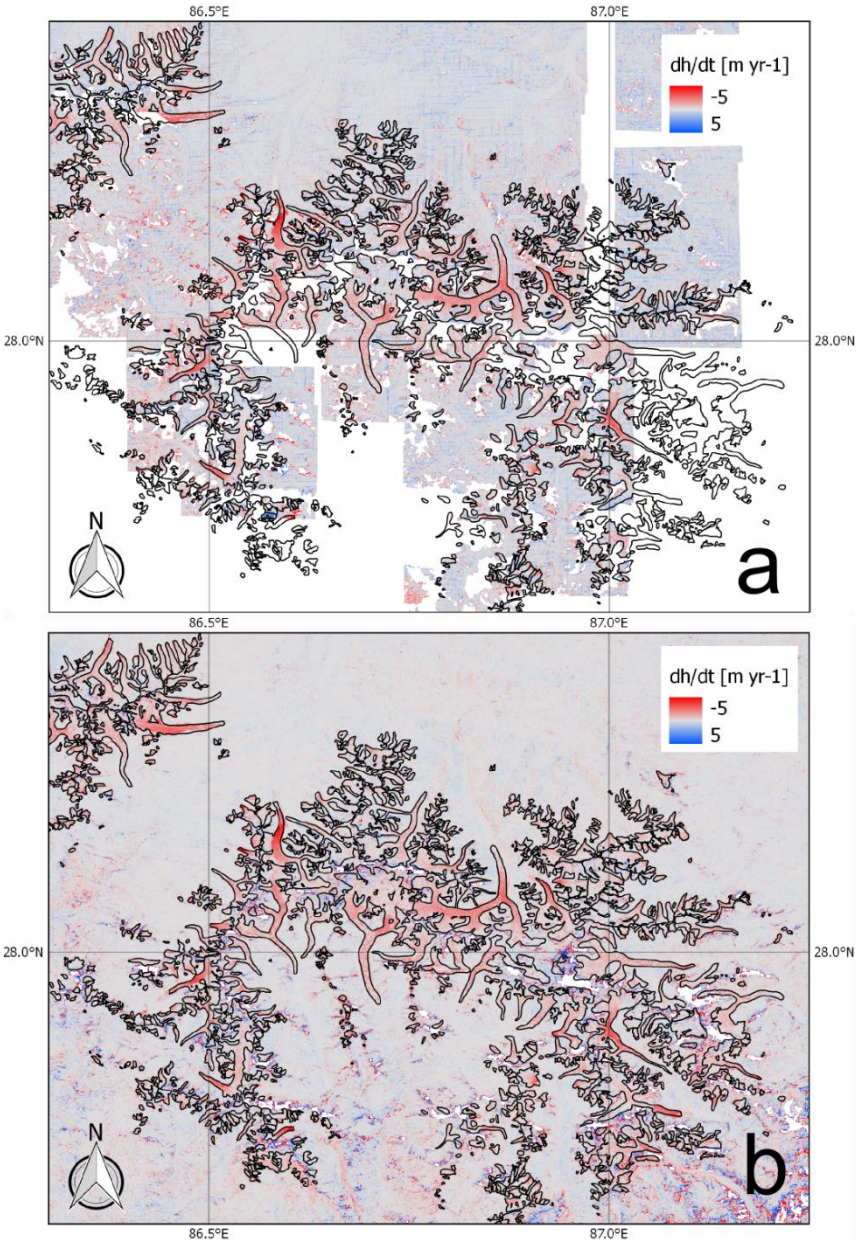

Figure S7: map of elevation change [m yr-1] for the period 2000-2016 over a subset of Everest region from ref.18 (a) and from this study (b).

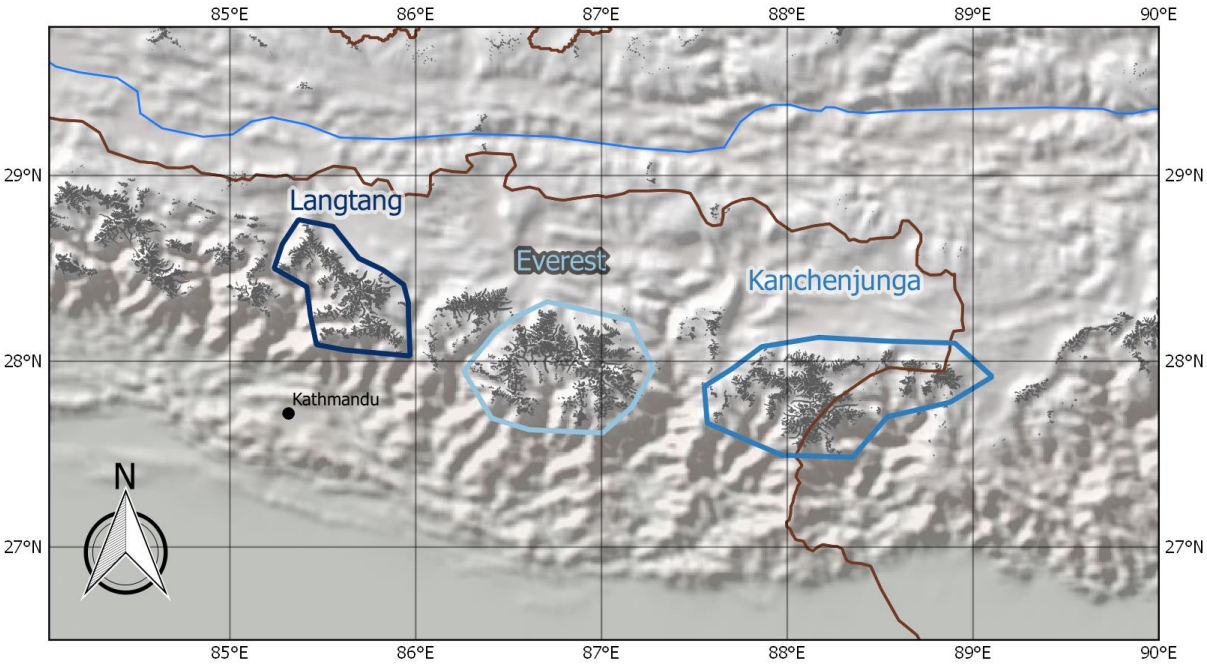

Figure S8: location of the three sub-regional studies discussed in the section "Spatial variability of individual glacier mass balances".

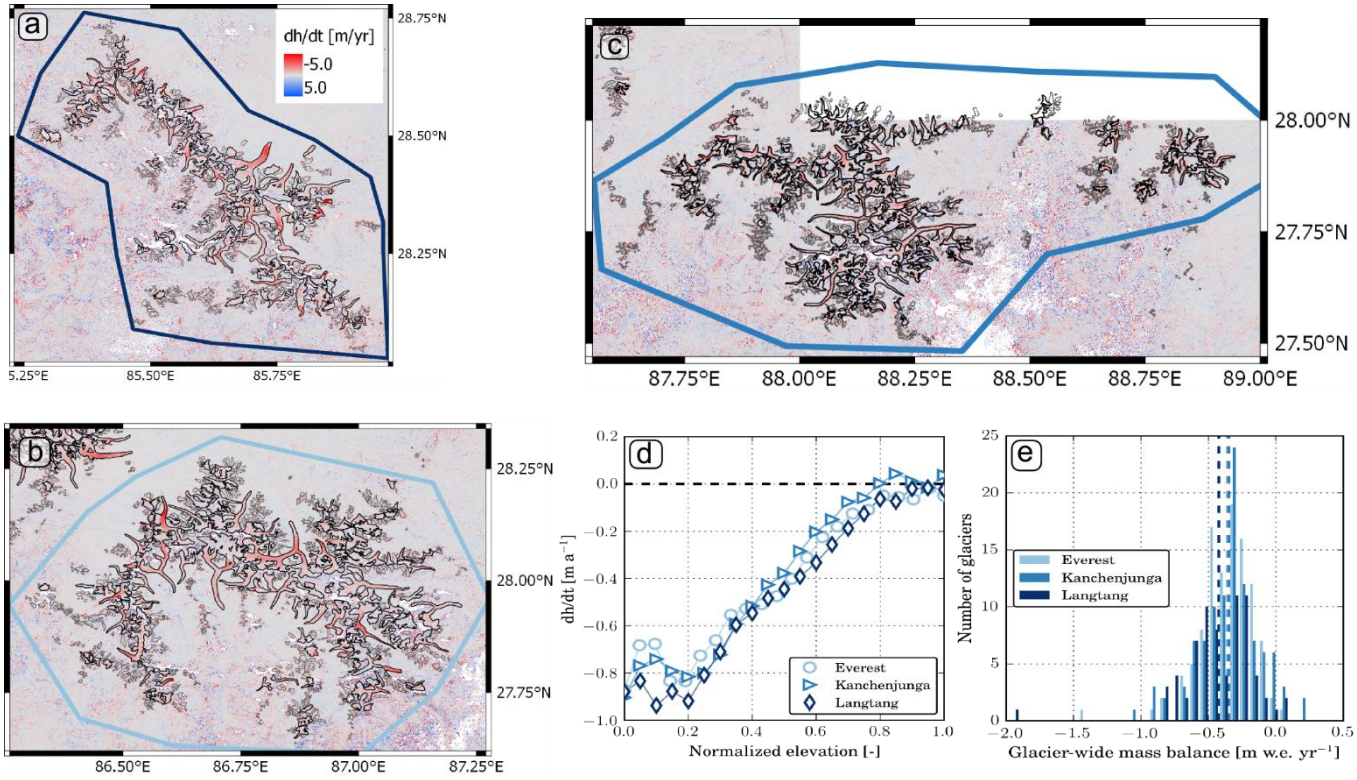

Figure S9: a, b, c- maps of rate of elevation change for Langtang, Everest, and Kanchenjunga, respectively. d- altitudinal distribution of thickness changes for the three sub-regions defined in Fig. S8 ; e- distribution of glacier-wide mass balances for individual glaciers larger than 2 km² and for which more than 70 % of the surface is classified as good data. The vertical dashed lines represent the sub-region-wide mass balances.

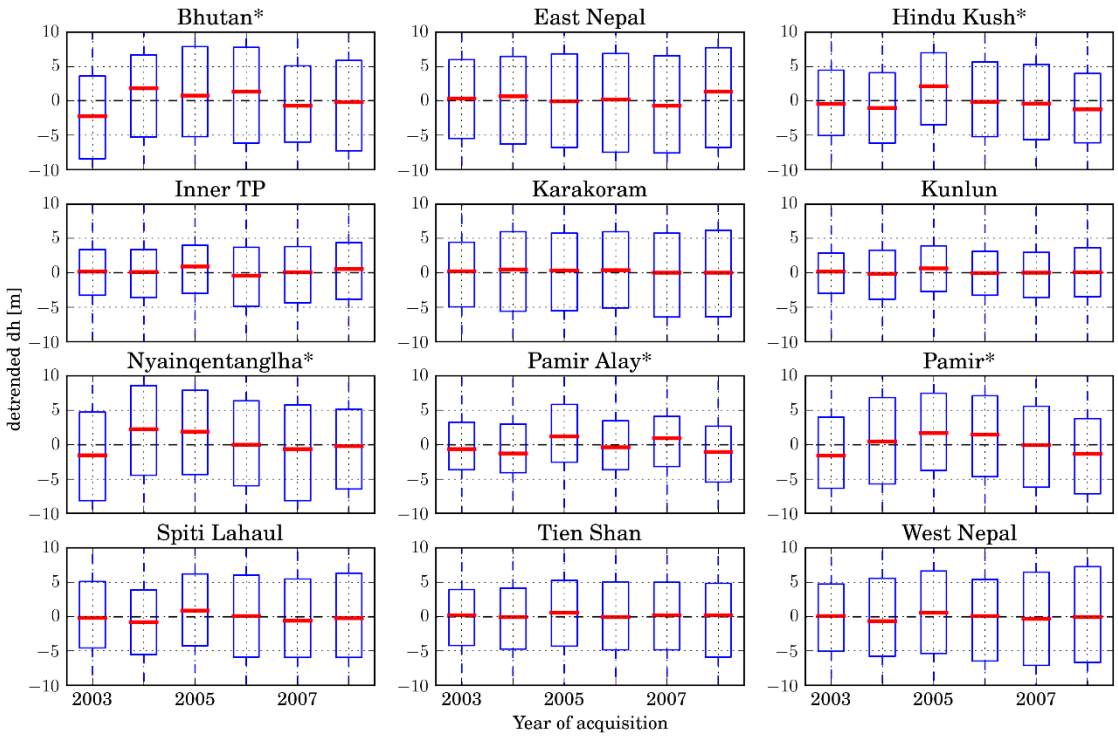

Figure S10: boxplots of the detrended ICESat dh (ICESat elevation – SRTM) grouped by year of acquisition. The controversial regions are marked with an asterisk.

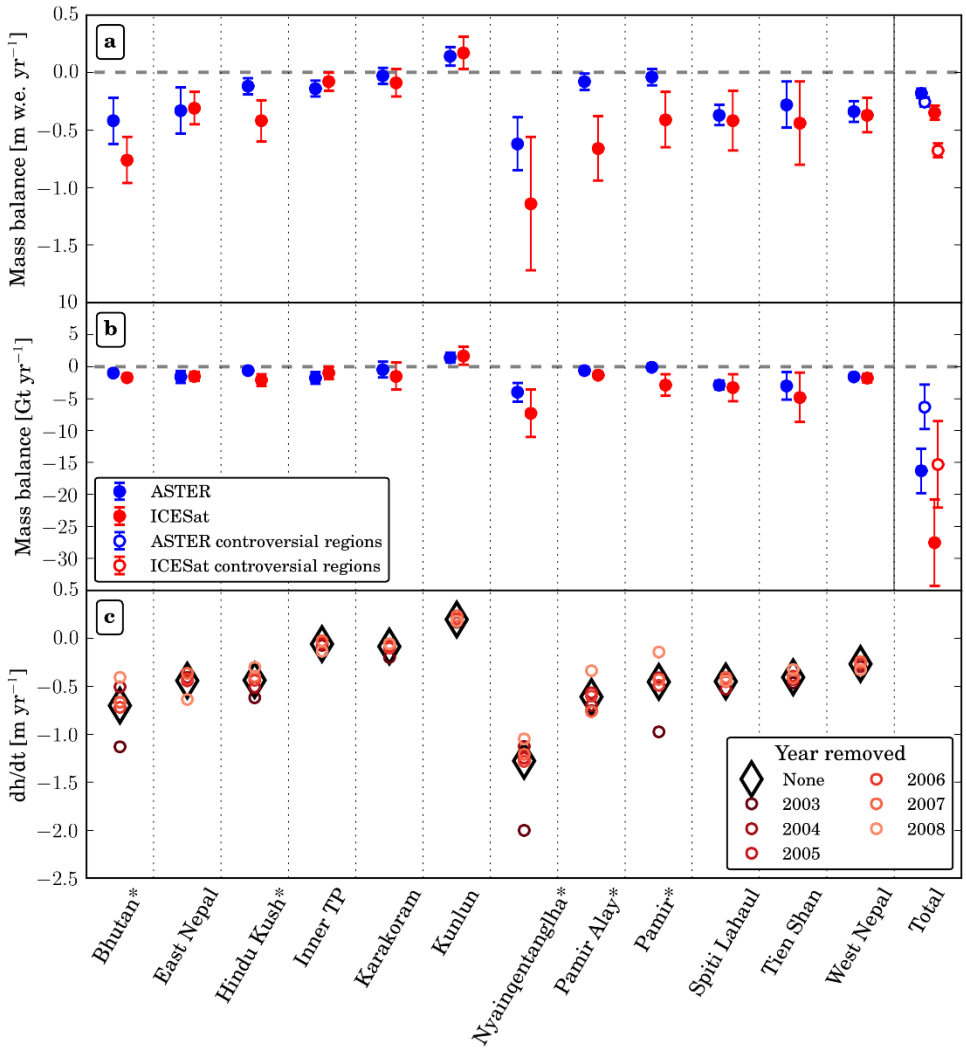

Figure S11: a- Region-wide specific mass balance (in m w.e. yr^{-1}) for each region; b- Region-wide mass balance (in Gt yr^{-1}) for each region; c- Results of the bootstrap test for each region. For a given region, the solid diamond represents the robust temporal fit through all ICESat dh (i.e. Elevation ICESat – SRTM) data and each of the colored circle represents the robust temporal fit of the ICESat dh excluding one year of acquisition. The controversial regions are marked with an asterisk.

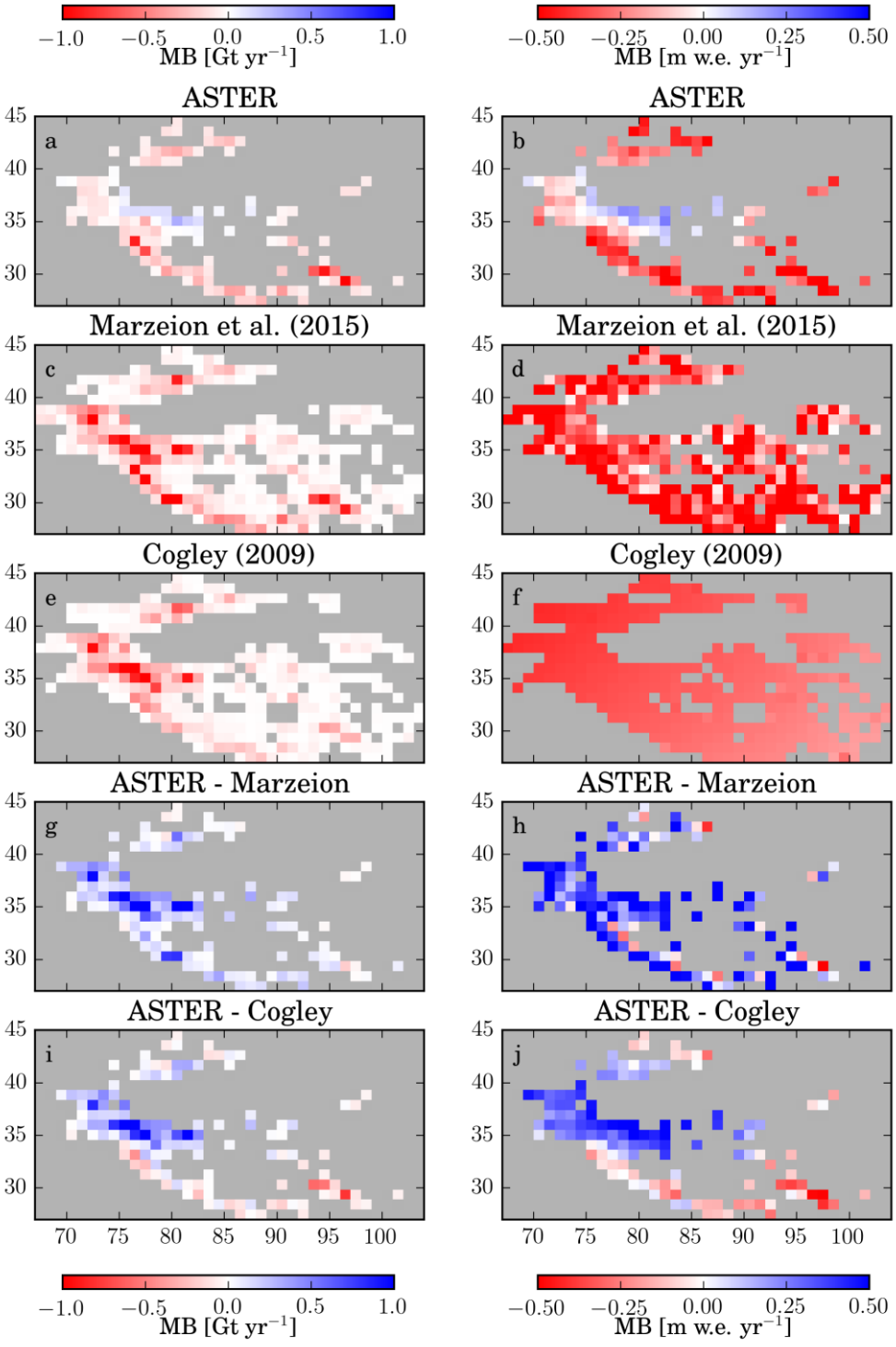

Figure S12: Mass balance in Gt yr^{-1} (a, c, e, g, i) and in m w.e. yr^{-1} (b, d, f, h, j) on a 1°×1° grid. Mass balance estimates are obtained from ASTER trends (a, b, this study), numerical modelling (c, d, Marzeion et al. 2015, ref. 26) and interpolation (e, f, Cogley 2009, ref. 27). g, h, i and j shows grid based comparisons of the different datasets.

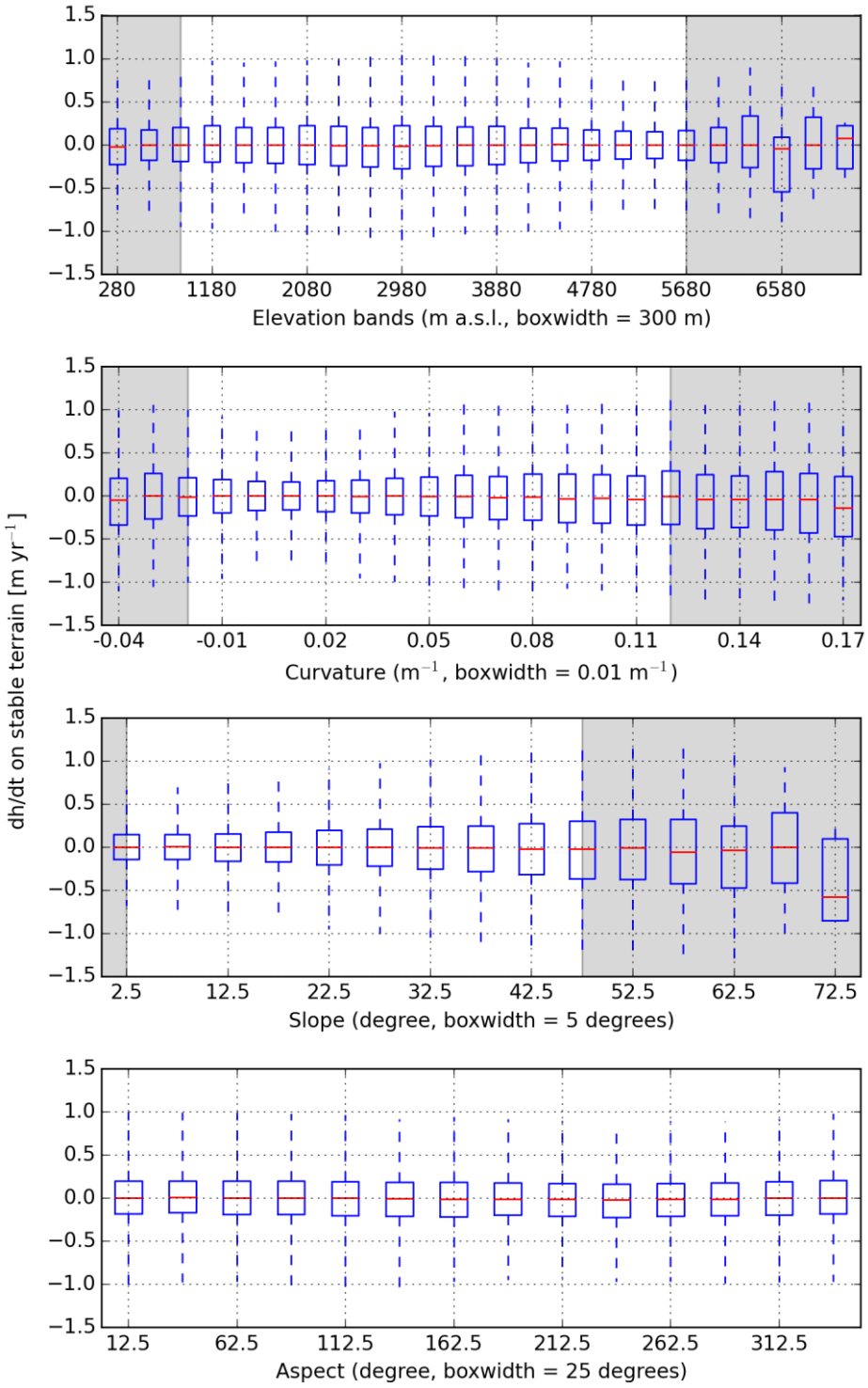

Figure S13: rate of elevation change (m yr^{-1}) on stable terrain for 132 000 randomly chosen points.

Supplementary references

1. Berthier, E. *et al.* Glacier topography and elevation changes derived from Pléiades sub-meter stereo images. *The Cryosphere* **8,** 2275–2291 (2014).
2. Huss, M. Density assumptions for converting geodetic glacier volume change to mass change. *The Cryosphere* **7,** 877–887 (2013).
3. Azam, M. F. *et al.* Meteorological conditions, seasonal and annual mass balances of Chhota Shigri Glacier, western Himalaya, India. *Ann. Glaciol.* **57,** 328–338 (2016).
4. Gardelle, J., Berthier, E. & Arnaud, Y. Impact of resolution and radar penetration on glacier elevation changes computed from DEM differencing. *J. Glaciol.* **58,** 419–422 (2012).
5. Bajracharya, S. R. & Shrestha, B. *The Status of Glaciers in the Hindu Kush-Himalayan Region*. (International Centre for Integrated Mountain Development, Kathmandu, Nepal, 2011).
6. Glaciers_cci consortium. Climate Research Data Package (CRDP) Technical Document. (2015).
7. Nuimura, T. *et al.* The GAMDAM glacier inventory: a quality-controlled inventory of Asian glaciers. *The Cryosphere* **9,** 849–864 (2015).
8. Paul, F. *et al.* On the accuracy of glacier outlines derived from remote-sensing data. *Ann. Glaciol.* **54,** 171–182 (2013).
9. Pfeffer, W. T. *et al.* The Randolph Glacier Inventory: a globally complete inventory of glaciers. *J. Glaciol.* **60,** 537–552 (2014).
10. Kääb, A., Treichler, D., Nuth, C. & Berthier, E. Brief Communication: Contending estimates of 2003-2008 glacier mass balance over the Pamir–Karakoram–Himalaya. *The Cryosphere* **9,** 557–564 (2015).
11. Treichler, D. & Kääb, A. ICESat laser altimetry over small mountain glaciers. *The Cryosphere* **10,** 2129–2146 (2016).
12. Pohl, E., Gloaguen, R., Andermann, C. & Knoche, M. Glacier melt buffers river runoff in the Pamir Mountains. *Water Resour. Res.* **53,** 2467–2489

13. Yi, S. & Sun, W. Evaluation of glacier changes in high-mountain Asia based on 10 year GRACE RL05 models. *J. Geophys. Res. Solid Earth* **119,** 2504–2517 (2014).
14. Barandun, M. *et al.* Re-analysis of seasonal mass balance at Abramov glacier 1968-2014. *J. Glaciol.* **61,** 1103–1117 (2015).
15. Gardelle, J., Berthier, E., Arnaud, Y. & Kääb, A. Region-wide glacier mass balances over the Pamir-Karakoram-Himalaya during 1999-2011. *The Cryosphere* **7,** 1263–1286 (2013).
16. Bolch, T., Pieczonka, T. & Benn, D. I. Multi-decadal mass loss of glaciers in the Everest area (Nepal Himalaya) derived from stereo imagery. *The Cryosphere* **5,** 349–358 (2011).
17. Nuimura, T., Fujita, K., Yamaguchi, S. & Sharma, R. R. Elevation changes of glaciers revealed by multitemporal digital elevation models calibrated by GPS survey in the Khumbu region, Nepal Himalaya, 1992-2008. *J. Glaciol.* **58,** 648–656 (2012).
18. King, O., Quincey, D. J., Carrivick, J. L. & Rowan, A. V. Spatial variability in mass loss of glaciers in the Everest region, central Himalayas, between 2000 and 2015. *The Cryosphere* **11,** 407–426 (2017).
19. Neckel, N., Kropáček, J., Bolch, T. & Hochschild, V. Glacier mass changes on the Tibetan Plateau 2003–2009 derived from ICESat laser altimetry measurements. *Environ. Res. Lett.* **9,** 014009 (2014).
20. Rankl, M. & Braun, M. Glacier elevation and mass changes over the central Karakoram region estimated from TanDEM-X and SRTM/X-SAR digital elevation models. *Ann. Glaciol.* **57,** 273–281 (2016).
21. Neckel, N., Loibl, D. & Rankl, M. Recent slowdown and thinning of debris-covered glaciers in south-eastern Tibet. *Earth Planet. Sci. Lett.* **464,** 95–102 (2017).
22. Pieczonka, T., Bolch, T., Junfeng, W. & Shiyin, L. Heterogeneous mass loss of glaciers in the Aksu-Tarim Catchment (Central Tien Shan) revealed by 1976 KH-9 Hexagon and 2009 SPOT-5 stereo imagery. *Remote Sens. Environ.* **130,** 233–244 (2013).

23. Gardner, A. S. *et al.* A Reconciled Estimate of Glacier Contributions to Sea Level Rise: 2003 to 2009. *Science* **340,** 852–857 (2013).
24. Vijay, S. & Braun, M. Elevation Change Rates of Glaciers in the Lahaul-Spiti (Western Himalaya, India) during 2000–2012 and 2012–2013. *Remote Sens.* **8,** 1038 (2016).
25. Ragettli, S., Bolch, T. & Pellicciotti, F. Heterogeneous glacier thinning patterns over the last 40 years in Langtang Himal, Nepal. *The Cryosphere* **10,** 2075–2097 (2016).
26. Marzeion, B., Leclercq, P. W., Cogley, J. G. & Jarosch, A. H. Brief Communication: Global reconstructions of glacier mass change during the 20th century are consistent. *The Cryosphere* **9,** 2399–2404 (2015).
27. Cogley, J. G. Geodetic and direct mass-balance measurements: comparison and joint analysis. *Ann. Glaciol.* **50,** 96–100 (2009).
28. Bolch, T., Buchroithner, M., Pieczonka, T. & Kunert, A. Planimetric and volumetric glacier changes in the Khumbu Himal, Nepal, since 1962 using Corona, Landsat TM and ASTER data. *J. Glaciol.* **54,** 592–600 (2008).
29. Farinotti, D. *et al.* Substantial glacier mass loss in the Tien Shan over the past 50 years. *Nat. Geosci* **8,** 716–722 (2015).
30. Yi, S., Wang, Q., Chang, L. & Sun, W. Changes in Mountain Glaciers, Lake Levels, and Snow Coverage in the Tianshan Monitored by GRACE, ICESat, Altimetry, and MODIS. *Remote Sens.* **8,** 798 (2016).